

# Growth of Nonlinear Patterns in Binary-Fluid Convection, Analysis of Models\*

C. Fütterer\*\*

Institut für Theoretische Physik, Universität des Saarlandes,  
Postfach 151150, 66041 Saarbrücken, Germany

Communicated by M.Y. Hussaini

Received 1 July 2002 and accepted 20 March 2003  
Published online 15 July 2003 – © Springer-Verlag 2003

**Abstract.** A recently proposed “minimal model” of the convection of binary mixtures in a Rayleigh–Bénard cell of aspect ratio 2 with realistic boundary conditions is invoked to study the transient dynamics from the entirely diffusive ground state to the convection state. The model was designed to reproduce the subcritical Hopf bifurcation found for negative Soret coupling in finite-difference simulations and experiments, but also performs well for the growth transients, including the competition between two counter-propagating waves. We prepared an initial state with only one wave, thus avoiding complicated wave competition. This allows us to elucidate the interaction of the concentration field with the pure-fluid fields, *i.e.*, temperature and velocity, by means of modulus and phase equations. We explain the linear and nonlinear transient dynamics responsible for the strong decrease in frequency and concentration, and the feed-back loop responsible for propagation.

## 1. Introduction

Convection in binary fluid mixtures is an exemplary system for pattern formation far from equilibrium and modeling (Cross and Hohenberg, 1993). This system has the advantage of being experimentally convenient (Walden *et al.*, 1985; Ohlsen *et al.*, 1990; Tounsi *et al.*, 1996; Ahlers and Rehberg, 1986; Liu and Ahlers, 1996, 1997; Gao and Behringer, 1986; Moses and Steinberg, 1988; Eaton *et al.*, 1991; Zimmermann and Müller, 1992; Winkler and Kolodner, 1992; La Porta *et al.*, 1996), where well-established equations allow a rigorous comparison of theoretical and experimental data (Barten *et al.*, 1989, 1990, 1995; Busse and Kramer, 1990; Bensimon *et al.*, 1989; Hollinger *et al.*, 1997; Knobloch and Moore, 1990; Lee *et al.*, 1983; Linz and Lücke, 1987; Linz *et al.*, 1988; Schöpf and Zimmermann, 1993; Veronis, 1965; Malomed and Nepomnyashchy, 1990; Fauve and Thual, 1990; van Saarloos and Hohenberg, 1990; Deissler and Brand, 1990; Riecke, 1992a,b, 1996; Landau and Lifschitz, 1996; Platten and Legros, 1984). Compared with convection in one-component fluids, the spatio-temporal structures in binary mixtures can be very complex due to: (i) the Soret coupling  $\psi$  responsible for concentration fluctuations; (ii) the different time scales of small dissipative solutal diffusion and fast temperature and momentum diffusion; and (iii) the competition between

---

\* This work has been supported by Deutsche Forschungs-Gemeinschaft and VW-Stiftung.

\*\* *Present address:* Laboratoire de Physico-Chimie, Institut Curie (UMR CNRS/IC 168), 26 Rue d’Ulm, 75248 Paris Cedex 05, France.

convection and mixing on one side and diffusion on the other (Cross and Hohenberg, 1993; Landau and Lifschitz, 1996; Lücke *et al.*, 1998). In addition to the pure fluid equations, the concentration field equation introduces the very large number of degrees of freedom needed to describe the phenomena discussed here. The concentration field is influenced by the velocity field (via the advection term) and by the temperature field (via the Soret term), whereas the concentration enters only the momentum balance via the solutal contribution to buoyancy, hence creating a feed-back loop. This feed-back loop is responsible for the wealth of patterns emerging from oscillatory and stationary instabilities (Hollinger *et al.*, 1998; Cross and Hohenberg, 1993).

This paper is focused on the two-dimensional transient convection structures with laterally periodic and vertically realistic boundary conditions studied previously with finite difference (FD) simulations (Lücke *et al.*, 1998; Fütterer, 1999; Fütterer and Lücke, 1999, 2000, 2002). We confine ourselves to the case  $\psi = -0.25$ , *i.e.*, positive temperature gradients causing negative concentration gradients. Consequently, the quiescent fluid state is stabilized by the concentration distribution concentrating the lighter fluid component near the upper plate. The concentration diffusion ( $L = 0.01$ ) is much smaller than the diffusion of the other fields (velocity  $\sigma = 10$ , temperature: scaled to 1), introducing a very long time scale. Hence, the slow concentration field for the most part passively follows the velocity and the temperature field. Only, if the thermal contribution to the buoyancy is large enough can the conductive state be destabilized. This mechanism is responsible for the backward folded bifurcation structure as well as the relatively late initialization of nonlinear phenomena during the transient evolution from the ground state to the convection state, the subject of the present publication. At the end the concentration is advectively imprisoned and mixed by the velocity field and its gradients strongly reduced (see Fütterer and Lücke, 2002). Additionally, the binary mixture convection shows *phase-shifts* between the fields yielding a stable propagation and a complex competition dynamics of two counter-propagating waves.

Much theoretical work has been done to understand and model (mainly nontransient) patterns observed in experiments and simulations, in particular, traveling waves (TWs) and their origin in relation to the Soret effect (Veronis, 1965; Cross, 1986; Ahlers and Lücke, 1987; Linz *et al.*, 1988; Bensimon *et al.*, 1989). Modeling of the backward folded bifurcation branch for negative  $\psi$  was successfully described for the first time by the “minimal Galerkin model” in Hollinger *et al.*, (1998) and Lücke *et al.*, (1998). This model, initially derived to study relaxed nonlinear structures, has been adapted for time-dependent numerical solutions (fourth-order Runge–Kutta code) to study the transition from the ground state to the nonlinear convective state. Emphasis is placed on the interaction between the different terms, as well as the relation to the results of FD simulations presented in Fütterer and Lücke, (2002). We elucidate the linear and nonlinear growth, the mechanisms responsible for TW propagation, and the drastic decrease of the concentration amplitude and the propagation velocity during relaxation into the fixed point by means of model analysis, focusing on the analysis of temporal behavior of the amplitudes and phases. In the present publication we restrict ourselves to the nonlinear growth of *one* TW. However, the situation for realistic initial conditions is more complicated due to the additional competition of two counter-propagating waves.

## 2. System

We consider a binary fluid layer of mean temperature  $\bar{T}$  and mean concentration  $\bar{C}$ . The concentration field measures the lighter component. It is confined between two perfectly heat conducting, impermeable, horizontal plates and exposed to a vertical gravitational acceleration  $g$  and to a vertical temperature gradient  $\Delta T/d$  directed from top to bottom, where  $d$  is the layer thickness.

The balance equations for mass, momentum, heat, and concentration (Landau and Lifschitz, 1966; Platten and Legros, 1984) in Oberbeck–Boussinesq approximation (Barten *et al.*, 1995) are

$$0 = -\nabla \cdot \mathbf{u}, \quad (1)$$

$$\partial_t \mathbf{u} = -(\mathbf{u} \cdot \nabla) \mathbf{u} - \nabla \left[ p + \left( \frac{d^3}{\kappa^2} g \right) z \right] + \sigma \nabla^2 \mathbf{u} + R\sigma (T + C) \mathbf{e}_z, \quad (2)$$

$$\partial_t T = -\nabla \cdot \mathbf{Q} = -\nabla \cdot [\mathbf{u}T - \nabla T], \quad (3)$$

$$\partial_t C = -\nabla \cdot \mathbf{J} = -\nabla \cdot [\mathbf{u}C - L\nabla (C - \psi T)]. \quad (4)$$

Here,  $T$  and  $C$  denote deviations of the temperature and concentration fields, respectively, from their global mean values  $\bar{T}$  and  $\bar{C}$ , and  $\mathbf{Q}$  and  $\mathbf{J}$  are the associated currents. The Dufour effect (Hort *et al.*, 1992; Hollinger and Lücke, 1995), which couples the concentration gradients into the heat current  $\mathbf{Q}$  is discarded in (3), since it is relevant only in few binary gas mixtures (Liu and Ahlers, 1996, 1997) and in liquids near the liquid–vapor critical point (Lee *et al.*, 1983).

Besides the Rayleigh number  $R = \alpha g d^3 / \nu \kappa \Delta T$  measuring the thermal drive of the fluid, three additional numbers enter the field equations (1)–(4): the Prandtl number  $\sigma = \nu / \kappa$ , the Lewis number  $L = D / \kappa$ , and the separation ratio or Soret constant  $\psi = -\beta k_T / \alpha \bar{T}$ . The latter characterizes the sign and the strength of the Soret effect. Negative Soret coupling  $\psi$ , as we always assume here, induces concentration gradients antiparallel to temperature gradients. In this situation the buoyancy induced by solutal changes in density is opposed to the thermal buoyancy. We consider mixtures like ethanol–water, for which  $L = 0.01$ ,  $\sigma = 10$ , and  $\psi = -0.25$ , that are easily accessible experimental parameters. We use the reduced Rayleigh number  $r = R / R_c^0$  scaled by the critical Rayleigh number  $R_c^0$  for the onset of pure-fluid convection with the critical wave number  $k_c^0$ . The analytical values are  $R_c^0 = 1707.762$  and  $k_c^0 = 3.11632$ . To compare our FD numerical results with experimental, analytical, or numerical ones, we scale  $R$  by the threshold  $R_c^0$  of our code with uniform spatial resolution of  $\Delta = 1/20$ ,  $R_c^0 = 1685.8$  (Jung, 1997). All our FD results, which served as a reference for developing the model, refer to this resolution.

When the total buoyancy exceeds a threshold, convection sets in – typically in the form of straight rolls for negative  $\psi$ . Ignoring field variations along the roll axes we describe here two-dimensional convection in an  $x$ – $z$  plane perpendicular to the roll axes, with a velocity field

$$\mathbf{u}(x, z, t) = u(x, z, t) \mathbf{e}_x + w(x, z, t) \mathbf{e}_z. \quad (5)$$

This two-dimensional<sup>1</sup> type of convection is commonly enforced experimentally in convection channels of small extension in the  $y$ -direction since the rolls are more stable if oriented perpendicular to the channel walls (Davis, 1967; Cross, 1982).

To find the time-dependent solutions of the partial differential equations (1)–(4) describing convection, we performed numerical simulations with an FD code (Welch *et al.*, 1965; Barten *et al.*, 1990; Hirt *et al.*, 1975). The boundary conditions for the fields were as follows: realistic no slip conditions for the top and bottom plates at  $z = \pm \frac{1}{2}$ ,

$$\mathbf{u} \left( x, z = \pm \frac{1}{2}; t \right) = 0, \quad (6)$$

and perfect heat conducting plates connected to two heat reservoirs:

$$T \left( x, z = \pm \frac{1}{2}; t \right) = \mp \frac{1}{2}. \quad (7)$$

Furthermore, impermeability of the horizontal boundaries for the concentration was guaranteed by enforcing that the vertical concentration current  $\mathbf{e}_z \cdot \mathbf{J}$  vanishes at both plates:

$$\mathbf{e}_z \cdot \mathbf{J} = -L \partial_z (C - \psi T) \left( x, z = \pm \frac{1}{2}; t \right) = 0. \quad (8)$$

We restricted our investigation to one-dimensional *extended* convection structures. Consequently, lateral periodicity was imposed in the  $x$ -direction with periodicity length  $\lambda = 2\pi/k = 2$ . The associated wave number  $k = \pi$  is close to the critical wave number,  $k_c = 3.12$ , for the negative Soret coupling  $\psi = -0.25$  investigated here.

<sup>1</sup> Note: two-dimensional convection generates a one-dimensional pattern.

### 3. Minimal Galerkin Model

The analysis of the relaxed TW states obtained by a FD simulations permits the extraction of the essential modes necessary for a Galerkin approximation without distorting the shape of the bifurcation branch too much (Hollinger *et al.*, 1998). The minimal model contains seven modes, of which four are complex and three are real. Modes having an  $x$ -dependence need to be complex since the phase is associated to the lateral position. The velocity field and the temperature field are sufficiently expressed by one and two modes, respectively, as known from the Lorenz model.

The stream function is used to reduce the dimension of the velocity field, assuming incompressibility of the fluid:

$$\phi(x, z, t) = \frac{i}{k} X'_1(t) e^{-ikx} \frac{1}{2} [1 + \cos(2\pi z)] + \text{c.c.}$$

from which the corresponding velocity field  $(u, w)$  can be obtained by  $[u(x, z, t), w(x, z, t)] = (-\partial_z, \partial_x) \phi(x, z, t) + \text{c.c.}$  The temperature field is

$$T(x, z, t) = -z + Z'(t) \sqrt{2} \sin(2\pi z) + Y'(t) \sqrt{2} e^{-ikx} \cos(\pi z) + \text{c.c.}$$

The term proportional to  $z$  is due to the external heat-flow through the system which drives the fluid layer out of equilibrium. Besides the Fourier modes needed for the complex concentration profiles, a particularly important ingredient of the model has been introduced into the concentration field (Hollinger *et al.*, 1998): a “ramp” mode  $\sim z$  describing its initial profile for which the impermeability condition, together with the Soret term, are responsible.

The set of minimal modes describing the concentration field are

$$\begin{aligned} C(x, z, t) = & V_0(t)z \\ & + V'_1(t) \sqrt{2} \sin(2\pi z) \\ & + V'_2(t) \sqrt{2} \sin(4\pi z) \\ & + U'_1(t) \sqrt{2} e^{-ikx} + \text{c.c.} \\ & + U'_2(t) \sqrt{2} e^{-ikx} \cos(2\pi z) + \text{c.c.} \end{aligned} \quad (9)$$

The minimal model is a compromise between compactness and a physically correct description in the sense that concessions have been made concerning the boundary condition of the concentration field to keep this minimal model as small as possible. The correct von-Neumann boundary condition of the concentration field, (8), would transform into a partial differential equation,  $V_0(t) = \partial_z C|_{\text{boundary}} + 2\pi \sqrt{2} V'_1(t) - 4\pi \sqrt{2} V'_2(t)$ . To avoid these complications, we weaken the boundary condition and consider only the *laterally averaged form*, which is identical to the Nusselt number,  $N$ ,  $(-1/\psi) \langle \partial_z C|_{\text{boundary}} \rangle_x = \langle \partial_z T|_{\text{boundary}} \rangle_x = N$ , which varies only weakly during the growth dynamics. Thus, as a reasonable approximation,  $N = 1$  is assumed, leading to the useful expression  $V_0(t) = -\psi + 2\pi \sqrt{2} V'_1(t) - 4\pi \sqrt{2} V'_2(t)$  (Hollinger *et al.*, 1998).

After appropriate rescaling,

$$\begin{aligned} X &= \frac{8}{5\pi^2} X', & Y &= \frac{6\pi\sqrt{2}}{5} rY', & Z &= \frac{6\pi\sqrt{2}}{5} rZ', \\ V_1 &= \frac{256\sqrt{2}}{15\pi} rV'_1, & V_2 &= \frac{256\sqrt{2}}{5\pi} rV'_2, \\ U_1 &= \frac{32\sqrt{2}}{5} rU'_1, & U_2 &= \frac{32\sqrt{2}}{5} rU'_2, \end{aligned}$$

and  $\tilde{\sigma} = \frac{27}{14} \sigma$ ,  $t \rightarrow t/2\pi^2$ , we obtain the minimal Galerkin model (Hollinger *et al.*, 1998),

$$\begin{aligned}\dot{X} &= -\tilde{\sigma}(X - Y) + \tilde{\sigma} \left[ \frac{9}{256} \pi^2 (2U_1 + U_2) \right], \\ \dot{Z} &= -2Z + (YX^* + \text{c.c.}), \\ \dot{Y} &= -Y + rX - XZ, \\ \dot{V}_1 &= L \left( -\frac{6}{5} V_1 + \frac{256}{15\pi^2} \psi Z - \frac{32}{15} V_2 \right) + \frac{1}{2} \left( U_1 X^* + \frac{7}{3} U_2 X^* + \text{c.c.} \right), \\ \dot{V}_2 &= L \left( -\frac{24}{5} V_2 + \frac{256}{15\pi^2} \psi Z - \frac{6}{5} V_1 \right) + \frac{1}{2} \left( U_1 X^* + 4U_2 X^* + \text{c.c.} \right), \\ \dot{U}_1 &= -\frac{1}{2} L U_1 + \frac{32}{3\pi^2} L \psi Y + \left( \psi r - \frac{45}{256} \pi^2 V_1 + \frac{5\pi^2}{64} V_2 \right) X, \\ \dot{U}_2 &= -\frac{5}{2} L U_2 + \frac{64}{9\pi^2} L \psi Y + \left( \psi r - \frac{15}{64} \pi^2 V_1 + \frac{5\pi^2}{128} V_2 \right) X,\end{aligned}\tag{10}$$

as a base for subsequent discussion.

The classical Lorenz model contained in (10) (the first three equations without  $U_1$  and  $U_2$ ) describes the Rayleigh–Bénard convection of pure liquids with the fixed points  $X^\infty = Y^\infty = e^{i\xi} \sqrt{\epsilon}$  and further  $Z^\infty = r - 1$ . The free arbitrary phase  $\xi$  expresses the translation invariance according to the periodic lateral boundary conditions. We introduce here the critical parameter  $\epsilon = r - 1$ . The modes are cross-coupled in an asymmetric manner: the pure fluid modes  $X, Y, Z$  all couple into the equations representing the concentration field, whereas the concentration modes couple back into the pure fluid “Lorenz sub-model” only by the buoyancy term (and in a specific way, as will be discussed).

Subsequently, the strong initial state dependence (see Fütterer and Lücke, 2002) is addressed first. Indeed, the minimal Lorenz model (as the full equations) linearly shows two complex eigenvalues representing two counter-propagating TWs as also observed in the FD solutions. If starting with a noisy initial state, both complex conjugate eigenvalues are typically represented as a superposition of these TWs which interact destructively. We prepare an initial state containing *only one* complex eigenvector representing the right-going TW to simplify the discussion of the points of interest in the frame of this publication: the mechanism of propagation, the decrease of propagation velocity, and the decrease of the concentration amplitude.

### 3.1. Selection of Initial Values and Comparison with FD Results

The full FD simulation revealed a strong initial value dependence of the growth dynamics, more precisely, on the ratio of the amplitudes of the right- ( $|R|$ ) and left-going waves ( $|L|$ ) (Fütterer, 1999; Fütterer and Lücke, 2002) leading to the definition of a determining asymmetry parameter

$$\eta = \frac{|R| - |L|}{|R| + |L|}.\tag{11}$$

The minimal Galerkin model reproduces this phenomenon. With our parameters, the linear eigenvalue spectrum of the model consists of two complex conjugate eigenvalues with positive real parts and real damped eigenvalues not considered further. In correspondence to (11), the solution can be written in the form

$$f(t) = e^{\gamma_0 t} \left( e^{i\omega_0 t} v_0 R + e^{-i\omega_0 t} v_0^* L \right)$$

with  $R$  and  $L$  being projections of the corresponding eigenvector and its complex conjugate on the initial-value vector and  $v_0$  depending on the projection matrix.  $\omega_0$  is the initial frequency, being the imaginary part of the corresponding eigenvalue. To impose values of  $\eta$ , appropriate values for the initial state can be chosen by solving the corresponding linear equation. The solutions of the minimal Galerkin model, with seven

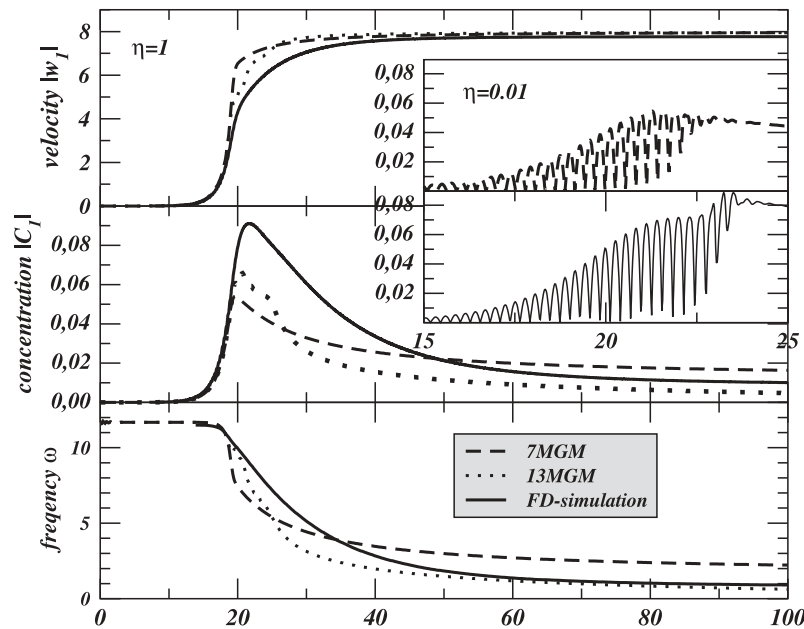


**Figure 1.** The evolution of the modulus of the first lateral Fourier mode of the velocity and the concentration field for two different models (7MGM and 13MGM) and the full FD solution with  $\eta = 1$  (pure right-going wave) and  $\eta = 0.01$  (random initial conditions) are shown. 7MGM switches abruptly from exponential growth to saturation, showing a kink in the velocity and the concentration field curve, whereas the FD solution reveals a smooth transition. 13MGM lies between both solutions. The FD concentration field further shows a much stronger overshoot than 7MGM or 13MGM. The fixed point of the concentration field solution of 7MGM shows too large values whereas the corresponding 13MGM curve is under the “correct” FD solution. The fluctuation of 13MGM shows that more modes are needed to reproduce the transient behavior correctly. The insert shows 7MGM and the FD solution of the concentration field for  $\eta = 0.01$ . The models, despite the compactness, are able to reproduce the competition of the right- and left-going wave, leading to the transition of an SW (standing wave) to a TW (traveling wave), very similar to the full simulation (Fütterer and Lücke, 2002). However, the details are not reproduced, i.e., the last dip after a short stagnation of the modulus oscillations (representing the SW). This is not astonishing when looking at the high spatio-temporal complexity of the transients as discussed extensively in Fütterer and Lücke, (2002).

modes (7MGM), and an extended Galerkin model, with 13 modes (13MGM), simulated with a fourth degree Runge–Kutta code, are presented in Figure 1 and compared with the FD solution. Qualitatively, the same behavior is observed as for the FD simulation presented in Fütterer and Lücke, (2002). However, since the Galerkin model has a rather limited phase space, it cannot reproduce all the details found in the FD simulation subsequently discussed.

We now briefly discuss different  $\eta$ 's; however, in the next sections we refer only to the pure TW. The initial condition  $\eta = \pm 1$  (Figure 1) yields a pure TW over the whole growth dynamics in the FD, as well as in the models, avoiding the interaction with the second wave complicating the situation enormously.

The 7MGM shows a long exponential growth phase followed by an abrupt transition (kink in the amplitude) from the saturation phase. This reflects the FD solution only qualitatively, since the shape of the curves are different and the amplitudes in the fixed points are more than two times too large. The lacking higher modes, necessary to create the complex mixing structures (Fütterer and Lücke, 2002), the large and flat concentration plateaus, and the steep gradients in the boundary layers (Barten *et al.*, 1995), are responsible for this discrepancy. The solution of the Galerkin model with an extension of the concentration sector approaches the (“exact”) FD solution. It is thereby essential when deriving the extended model with 13 modes (13MGM) that the buoyancy and the Soret term, the crucial parts of the feed-back loop, be extended by the *same* number of modes (Hollinger *et al.*, 1998). The extended model lies between the FD and the 7MGM solutions but the fixed point value of the concentration field is too small now. Further extensions would, without any doubt, allow us to reproduce more precisely the FD solution, however, the minimal model is more convenient to study the mechanisms behind the dynamics, the subject of this publication.

The lack of modes is particularly serious in the case of  $\eta = 0$ . The extremely abrupt transition from SW to SOC (Steady Overturning Convection) with a collapsing frequency, as found in the FD simulation (Fütterer

and Lücke, 2002), cannot be reproduced properly by the minimal model. Instead, at the beginning of the saturation phase we found a long decaying amplitude modulation. However, this case is somewhat artificial since it is unstable.

The value  $\eta = 0.01$  represents a generic scenario, which can be observed when using random initial conditions. It shows quite good agreement with the FD solution even if the details of the transition dynamics, as the overshooting, are not properly reproduced.

Concluding, the minimal model is very valuable to study qualitatively the mechanisms and interactions of the different terms and modes during the growth transients.

### 3.2. Mechanism of Propagation and Decrease of Frequency

In this section we discuss first the smallest “sub-model”, the Lorenz model being part of the minimal model for binary-mixture convection. Then we consider additional terms related to the concentration field with the goal to elucidate the propagation and frequency decrease.

The Lorenz model, describing pure fluid convection, shows initially, when starting with a slightly randomly disturbed conductive state, exponential growth and a saturation phase; finally the SOC fixed point is reached. The dynamics, disregarding a very short initial transient ( $\ll 1$  time unit), does *not* depend on the initial values provided they are small. The Euler notation,  $X(t) = |X(t)| e^{i\varphi_X(t)}$ ,  $Y(t) = |Y(t)| e^{i\varphi_Y(t)}$ , is convenient to study phase dynamics. We obtain

$$\dot{\varphi}_X = a_X \sin(\varphi_Y - \varphi_X), \quad (12)$$

$$\dot{\varphi}_Y = a_Y \sin(\varphi_X - \varphi_Y), \quad (13)$$

with the following abbreviations:

$$a_X = \tilde{\sigma} \frac{|Y|}{|X|}, \quad b_X = \tilde{\sigma} \frac{9\pi^2}{128} \frac{|U_1|}{|X|}, \quad \text{and} \quad a_Y = (r - Z) \frac{|X|}{|Y|}. \quad (14)$$

These equations clearly show that the difference  $\varphi_X(t) - \varphi_Y(t)$  always vanishes immediately and does not influence the subsequent linear and nonlinear dynamics. This explains why real equations are perfectly justified to study pure fluid convection.

However, the binary mixture equations introduce two additional terms into the velocity field equation of the pure fluid model. Only the first matters, since the second contribution containing the concentration mode  $U_2$  is, for our parameters, negligible. Consequently, the buoyancy leads to the additional term  $b_X \sin(\varphi_{U_1} - \varphi_X)$  contributing in (12). We anticipate that  $r - Z(t) \geq 0$  is always true for our parameters (which will be justified by (20)).

With

$$z = a_X e^{i\varphi_Y} + b_X e^{i\varphi_{U_1}} = |z| e^{i\zeta},$$

where  $z$  is the vector-sum and  $\zeta$  is its phase of the complex variables  $a_X e^{i\varphi_Y}$  and  $b_X e^{i\varphi_{U_1}}$ , (12) transforms into the easily interpretable form

$$\dot{\varphi}_X = \rho_X \sin(\zeta - \varphi_X).$$

Assuming constant  $\zeta$ , it is clear that, after all, the phase  $\varphi_X$  seeks to coincide with  $\zeta$  exactly like in (12). With decreasing  $\zeta - \varphi_X$ , the distance of  $\varphi_X$  to  $\varphi_Y$  increases and (13) comes into play pushing  $\varphi_Y$  toward  $\varphi_X$ . All three corresponding vectors align in the SOC fixed point and remain locked when changing  $\zeta$  slowly.

To establish permanent propagation, the concentration equation for the  $U_1$  mode in (10), comprising the Soret term, has to be taken into account. The phase of the first concentration mode follows the equation

$$\dot{\varphi}_{U_1} = \Psi \sin(\varphi_X - \varphi_{U_1}) \quad (15)$$

introducing the “effective Soret coefficient”

$$\Psi = \left( \psi r - \frac{45\pi^2}{256} V_1 + \frac{5\pi^2}{64} V_2 \right) \frac{|X|}{|U_1|}. \quad (16)$$

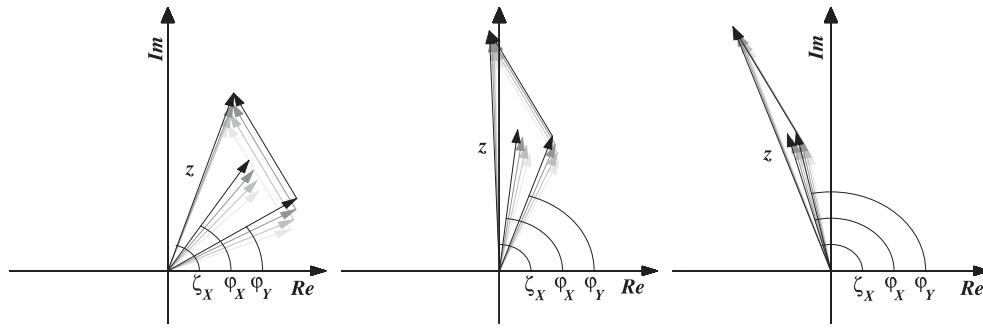


**Figure 2.** The Lorenz model with the phases  $\varphi_X$  and  $\varphi_Y$  mode and  $\zeta_X$  attempts to minimize phase differences as explained in the text. The Soret term counteracts and maintains the phase differences responsible for stable propagation of the structures. In this figure the relaxation of the phase differences as a function of not equilibrated initial conditions is shown. The dynamics is indicated by broken lines.

A second contribution in (15) showing very small values has been omitted. The “effective Soret coefficient”  $\Psi$  contains the Soret constant  $\psi$ , which is negative ( $\psi = -0.25$ ) in our case. As a result  $\Psi$  is initially equal to  $\psi r(|X|/|U_1|)$ , thus strongly negative, when assuming small initial values. Thus, the respective phase  $\varphi_{U_1}$  is pushed constantly away from  $\varphi_X$ , hence acting *against* the alignment mechanism described beforehand, and the triangle in Figure 2 remains wide open for a long time. This interplay of repulsion and attraction, finally, keeps the system away from the pure fluid stationary fixed point in favor of constantly rotating complex modes which correspond to permanent propagation of the fields. In a later state, if  $V_1$  and  $V_2$  have grown sufficiently,  $\Psi$  increases (approaching zero) and the destabilization becomes weaker, the triangle shrinks, and the propagation slows down, as was also observed in the full FD simulation.

Concluding, two mechanisms are balanced to maintain propagation: the buoyancy with a tendency to approach the phases and the negative Soret effect trying to increase the distance. A growing concentration amplitude weakens the second mechanism and consequently the propagation slows down. Nevertheless, this small set of equations is not sufficient to create an oscillatory fixed point. This is the reason why the  $U_2$  equation is needed: to maintain a very small phase shift at the end.

So far the phase dynamics elucidates the propagation of the structures. The modulus equations for the velocity field, represented by mode  $X$ , and the temperature field, represented by  $Y$  and  $Z$ , are

$$\partial|X|/\partial t = -\tilde{\sigma} [|X| - |Y| \cos(\varphi_Y - \varphi_X)] , \quad (17)$$

$$\partial Z/\partial t = 2 \{-1 + |X| |Y|/Z \cos(\varphi_X - \varphi_Y)\} Z , \quad (18)$$

$$\partial|Y|/\partial t = \{-1 + (r - Z) |X|/|Y| \cos(\varphi_X - \varphi_Y)\} |Y| . \quad (19)$$

As found in the preceding section, the phase differences are stabilized by the cooperation of the buoyancy and the Soret term (feed-back loop). These phase differences, however small, enter the cosine functions in (17)–(19), being less sensitive to variations of small arguments. As a result, the phase dynamics do not dramatically change the modulus dynamics, and the solution of the Lorenz equations for pure fluids is conserved in the minimal model. The exponential growth and the long transient saturation phase are inherited by the full Galerkin model.

It is remarkable that the change from exponential growth to saturation, *i.e.*, from linear to nonlinear behavior, sets in late and very fast. The reason is the different nature of the critical modes  $X$  and  $Y$  on one side and the linearly damped mode  $Z$  on the other side in (17)–(19). Namely, the latter is excited only when the quadratic term,  $|X| |Y|$ , introducing a growth rate twice as big as for the critical modes, has grown sufficiently to result in a sign change on the right side of (18). Therefore, the linear dynamics can survive for a long time, but the change to the nonlinear regime is very abrupt. Fast growing  $Z$  diminishes the effective growth rate in the braces in (19). Since (17) just describes the mode  $X$  following  $Y$ , the growth rates shrink drastically and vanish at the end. These mechanisms are also inherited by the full-sized Galerkin model.

The small “sub-model” allows us to make further statements about the relation of convection amplitude and propagation frequency which remain valid for the full model. The growth rates of the modulus are

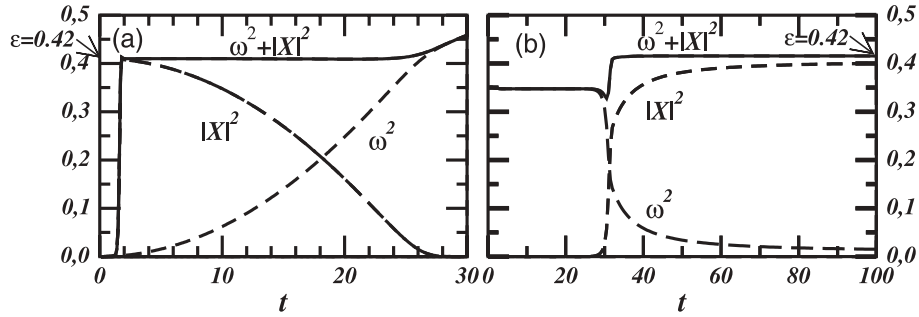


**Figure 3.** Test of (21). (a) The 7MGM has been modified in a way that an artificial and accelerating phase has been added to the phase of the velocity field. Only if the forced propagation exceeds  $\epsilon$  does the relation break down. (b) The growth of the patterns obtained from the FD simulation also satisfies the named relation during relaxation toward the fixed point.

smaller than their values, hence, (17) transforms approximately to  $|X| = |Y| \cos(\varphi_X - \varphi_Y)$  and (18) together with (19) yields  $Z = |X|^2$ . Finally, we get  $r - |X|^2 = 1/\cos^2(\varphi_X - \varphi_Y)$ , always being positive. Hence, we find an upper limit for the convection strength

$$|X|^2 \leq \epsilon. \quad (20)$$

Together with the relation  $\omega = \tilde{\sigma} \tan(\varphi_X - \varphi_Y)$  (Linz *et al.*, 1988) we finally obtain

$$|X|^2 + (\omega/\tilde{\sigma})^2 = \epsilon, \quad (21)$$

giving a simple relation between amplitude and frequency. This relation, (21), describes the reaction of the velocity amplitude on the propagation and has been tested by “pulling” artificially the temperature field by means of an additional linearly accelerating phase (Figure 3(a)). As soon as the convection amplitude vanishes, (21) fails. The “natural” dynamics of the full Galerkin model perfectly confirm this relation (Figure 3(b)) during the relaxation toward the fixed point (after approx.  $t = 32$  in Figure 3(b)) (Fütterer and Lücke, 2002) and represents a further property of binary mixtures inherited from simple fluids.

Since we always found  $\varphi_{U_1} - \varphi_X \approx \pi/2$  in our FD as well as in the 7MGM results, the equation of the first concentration-field mode in (15) can be reduced to

$$\Psi = \mp \omega \quad (22)$$

for right/left-going waves. The simulation of the Galerkin model confirmed this statement with very good satisfaction (a discrepancy of less than 1%), which allows the direct interpretation of the slowing down of the convection structures as a consequence of the fast increasing nonlinear modes  $V_1$  and  $V_2$ .

### 3.3. Decrease of Concentration Amplitude

The modulus equation for the concentration mode  $U_1$  is governed by

$$\partial|U_1|/\partial t = -\frac{1}{2}L|U_1| - \Psi|U_1|\cos(\varphi_X - \varphi_{U_1})$$

where an additional term, always being small, has been neglected. The solution is the exponent of the integral

$$-\frac{1}{2}L t + \int_0^t d\tau |\omega|(\tau) \cos(\varphi_X(\tau) - \varphi_{U_1}(\tau)) \quad (23)$$

showing the subtle balance between the diffusive term  $-\frac{1}{2}L t$  and the second term, implying the frequency  $\omega$  [using (22)] and the phase difference  $\varphi_X - \varphi_{U_1}$  from the advective term in the concentration equation. Contrary to the always small phase differences in the Lorenz part, this phase difference is slightly smaller than

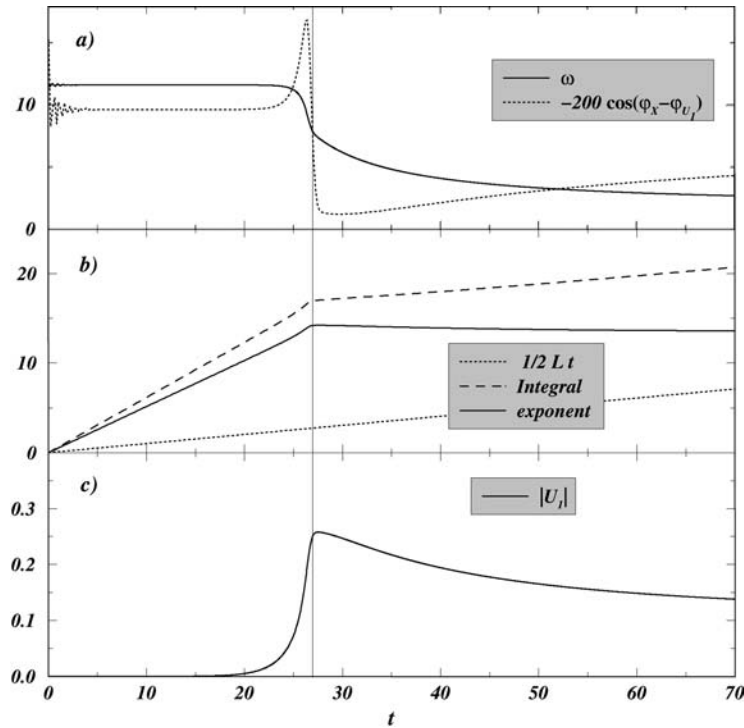


**Figure 4.** The subtle equilibrium between the diffusion and advection is disturbed by the nonlinear terms as soon as they enter the dynamics. Three terms are discussed to explain the shrinking concentration amplitude in the frame of the minimal Galerkin model: the diffusion proportional to  $L$ , the frequency  $\omega$ , and the phase difference between the  $X$ -mode representing the lateral velocity field and the first concentration mode  $U_1$ . In (a)  $\omega$  and  $-\cos(\varphi_X - \varphi_{U_1})$ , appropriately scaled, are both shrinking. As a result the values of the integral in (b) flatten and cease to overcompensate the diffusion contribution  $1/2Lt$ . The exponent decreases as shown in (b). Amplified by the exponential function we obtain the shape shown in (c).

$-\pi/2$  during the exponential growth and shifts toward  $-\pi/2$  during the subsequent transition to the nonlinear regime. The cosine function does *not* damp small deviations from  $\pi/2$  as is the case for deviations from a vanishing argument. During exponential growth the small negative value is multiplied by the large frequency value, and, as a consequence, overcomes the diffusive term. After the transition the cosine increases and gets very small. The growth of the integral slows down and gives priority to the constant diffusive contribution which finally predominates the dynamics in full agreement with the FD results (see also Fütterer and Lücke, 2002). Additionally, this change is amplified by the concomitant diminishing frequency. As a result the negative exponent in (23) and the amplitude  $|U_1|$  decrease, amplified by the exponential function (Figure 4).

In terms of the convection structures in space (Fütterer and Lücke, 2002), the small dephasing of the velocity field  $w$  relative to the concentration field during the evolution is essential for the equilibration of the concentration field. Initially, the phase shift of the vertical component of the velocity field and the concentration field is slightly smaller than  $\pi/2$ , allowing the convection rolls to pick up fluid with high/low concentration continuously from the top/bottom plate fluid (Fütterer and Lücke, 2002) thereby maintaining big concentration differences in the whole space. During the nonlinear competition this phase difference reduces and, as a consequence, less concentration is streaming inside the rolls. Hence, the concentration difference (concentration variance in Fütterer and Lücke, (2002)) is quickly mixed up and diffusively flattened, causing large concentration plateaus propagating slowly.

#### 4. Conclusion

The recently developed minimal Galerkin model for convection in binary mixtures was studied to elucidate the complex mutual influence of the concentration, velocity, and the temperature field during the growth dy-

namics. We explained the growth and propagation mechanism, the slowing down of the propagation, and the decreasing concentration amplitude, thereby rationalizing the observations discussed in Fütterer, (1999) and Fütterer and Lücke, (2002). The equations contain a complete Lorenz model describing pure fluid convection transferring many properties to the binary mixture equations.

We used the pure right TW initial condition to study the dynamics of the phase equations derived from the complex Lorenz model, avoiding the complicated competition with the left-going TW. As the first point, the propagation mechanism could be explained studying the phase and amplitude equations separately. However, the phases of the pure Lorenz equations coincide rapidly, leading to the well-known nonoscillatory SOC fixed point. Nevertheless, it could be derived that the sum of the squares of the system frequency (*i.e.*, the propagation velocity) and the convection amplitude are constant. This also proves to be true for the FD results and is inherited directly by the binary mixtures. Adding the inhomogeneity coming from the concentration field (buoyancy term), the phases of the other fields lock into the concentration phase. Adding the first concentration field equation, which contains the Soret term, we get two counter-acting “forces”, due to the buoyancy and the Soret term, acting as a feed-back loop. They eventually maintain stable propagation for a very long time. The vector representation of the modes in the complex plane visualizes these mechanisms. However, the seventh equation is needed to have a stable oscillatory fixed point.

The modulus equations of the Lorenz model elucidate the nonlinear dynamics related to the late but instantaneous frequency decrease: the nonlinearly excited mode  $Z$ , part of the temperature field, grows very late but twice as fast as the critical modes and slows down further growth of the critical modes.

Coming to the full model, we realized the following relations: The slowing down of the propagation (see (22) and (16)), depending initially only on the Soret coefficient, is finally compensated by the late but fast growing nonlinear concentration modes. The decrease of the concentration amplitude is caused by the balance of diffusion and advection (Fütterer and Lücke, 2002). The disappearing small phase shift combined with the decreasing propagation velocity favors diffusion over advection. This explains why the convection rolls are fed less by the boundary layers and why the enclosed concentration in the rolls get equilibrated with the result of a decrease of concentration variance in the system and plateau-formation (Fütterer and Lücke, 2002).

### Acknowledgment

I am particularly grateful to Prof. M. Lücke and St. Hollinger for numerous discussions.

### References

- Ahlers, G., and Lücke, M. (1987). Some Properties of an Eight-Mode Lorenz Model for Convection in Binary Fluids. *Phys. Rev. A*, **35**, 470.
- Ahlers, G., and Rehberg, I. (1986). Convection in a Binary Mixture Heated from Below. *Phys. Rev. Lett.*, **56**, 1373.
- Barten, W., Lücke, M., Hort, W., and Kamps, M. (1989). Fully Developed Traveling Wave Convection in Binary Fluid Mixtures. *Phys. Rev. Lett.*, **63**, 376.
- Barten, W., Lücke, M., and Kamps, M. (1990). Structure and Dynamics of Nonlinear Convective States in Binary Mixtures. In *Nonlinear Evolution of Spatio-Temporal Structures in Dissipative Continuous Systems* (F.H. Busse and L. Kramer, eds.). NATO ASI Series B2, vol. 225 p. 131, Plenum, New York.
- Barten, W., Lücke, M., Kamps, M., and Schmitz, R. (1995). Convection in Binary Fluid Mixtures. I. Extended Traveling-Wave and Stationary States. *Phys. Rev. E*, **51**, 5636.
- Bensimon, D., Pumir, A., and Shraiman, B.I. (1989). Nonlinear Theory of Traveling Wave Convection in Binary Mixtures. *J. Phys. (France)*, **50**, 3089.
- Busse, F.H., and Kramer, L. (eds.) (1990). *Nonlinear Evolution of Spatio-Temporal Structures in Dissipative Continuous Systems*, NATO ASI Series B2, vol. 225. Plenum, New York.
- Cross, M.C. (1982). Boundary conditions on the envelope function of convective rolls close to onset. *Phys. Fluids*, **25**, 936.
- Cross, M.C. (1986). An Eight-Mode Lorenz-Model of Traveling Waves in a Binary Fluid Convection. *Phys. Lett. A*, **119**, 21.
- Cross, M.C., and Hohenberg, P.C. (1993). Pattern Formation Outside of Equilibrium. *Rev. Mod. Phys.*, **65**, 851.
- Davis, S.H. (1967). Convection in a box: linear theory. *J. Fluid Mech.*, **30**, 465.
- Deissler, R.J., and Brand, H.R. (1990). The Effect of Nonlinear Gradient Terms on Localized States near a Weakly Inverted Bifurcation. *Phys. Lett. A*, **146**, 252.
- Eaton, K.D., Ohlsen, D.R., Yamamoto, S.Y., Surko, C.M., Barten, W., Lücke, M., Kamps, M., and Kolodner, P. (1991). Concentration Field in Traveling-Wave and Stationary Convection in Fluid Mixtures. *Phys. Rev. A*, **43**, 7105.

- Fauve, S., and Thual, O. (1990). Solitary Waves Generated by Subcritical Instabilities in Dissipative Systems. *Phys. Rev. Lett.*, **64**, 282.
- Fütterer, C. (1999). Transiente Konvektionsstrukturen in binären Fluidmischungen, Ph.D. thesis. Universität des Saarlandes, Saarbrücken.
- Fütterer, C., and Lücke, M. (1999). Initial-Growth Dependence of Convection Patterns in Pure Fluids and in Binary Mixtures. *Entropie*, **218**, 27.
- Fütterer, C., and Lücke, M. (2000). Growth of convection and boundary layers in binary mixtures. *J. Mol. Liq.*, **84**, 141.
- Fütterer, C., and Lücke, M. (2002). Growth of binary fluid convection: role of the concentration field. *Phys. Rev. E*, **65**, 36315-1.
- Gao, H., and Behringer, R.P. (1986). Convective Instabilities of a Normal Liquid  $^3\text{He}$ - $^4\text{He}$  Mixture. *Phys. Rev. A*, **34**, 697.
- Hirt, C.W., Nichols, B.D., and Romero, N.C. (1975). Sola – a Numerical Solution Algorithm for Transient Fluid Flow. Report LA-5852 Los Alamos Scientific Laboratory of the University of California.
- Hollinger, St., Büchel, P., and Lücke, M. (1997). Bistability of Slow and Fast Traveling Waves in Fluid Mixtures. *Phys. Rev. Lett.*, **78**, 235.
- Hollinger, St., and Lücke, M. (1995). Influence of the Dufour Effect on Convection in Binary Gas Mixtures. *Phys. Rev. E*, **52**, 642.
- Hollinger, St., Lücke, M., and Müller, H.W. (1998). Minimal quantitative model for the convection in binary liquids. *Phys. Rev. E*, **57**, 4250.
- Hort, W., Linz, S.-J., and Lücke, M. (1992). Onset of Convection in Binary Gas Mixtures: The Role of the Dufour Effect. *Phys. Rev. A*, **45**, 3737.
- Jung, Ch. (1997). Numerische Simulationen dreidimensionaler Konvektionsstrukturen in binären Fluiden mit positiver Soretkopplung, Ph.D. thesis. Universität des Saarlandes, Saarbrücken.
- Knobloch, E. and Moore, D.R. (1990). Nonlinear convection in binary mixtures. In *Nonlinear Evolution of Spatio-Temporal Structures in Dissipative Continuous Systems* (F.H. Busse and L. Kramer, eds.), pp. 109. NATO ASI Series B2, vol. 225. Plenum, New York.
- La Porta, A., Eaton, K.D., and Surko, C.M. (1996). Transition between Curved and Angular Textures in Binary Fluid Convection. *Phys. Rev. E*, **53**, 570.
- Landau, L. D., and Lifschitz, E.M. (1966). *Hydrodynamik*. Akademie-Verlag, Berlin.
- Lee, G.W.T., Lucas, P., and Tyler, A. (1983). Onset of Rayleigh-Bénard Convection in Binary Liquid Mixtures of  $^3\text{He}$  in  $^4\text{He}$ . *J. Fluid Mech.*, **135**, 235.
- Linz, S.J., and Lücke, M. (1987). Convection in Binary Mixtures: A Galerkin Model with Impermeable Boundary Conditions. *Phys. Rev. A*, **35**, 3997. Erratum: *Phys. Rev. A*, **36**, 2486 (1988).
- Linz, S.J., Lücke, M., Müller, H.W., and Niederländer, J. (1988). Convection in Binary Fluid Mixtures: Traveling Waves and Lateral Currents. *Phys. Rev. A*, **38**, 5727.
- Liu, J.L., and Ahlers, G. (1996). Spiral-Defect Chaos in Rayleigh-Bénard Convection with Small Prandtl Numbers. *Phys. Rev. Lett.*, **77**, 3126.
- Liu, J.L., and Ahlers, G. (1997). Rayleigh-Bénard Convection in binary-gas mixtures: Thermophysical properties and onset of convection. *Phys. Rev. E*, **55**, 6950.
- Lücke, M., Barten, W., Büchel, P., Fütterer, C., Hollinger, St., and Jung, Ch. (1998). Pattern formation in binary fluid convection and in systems with throughflow. In *Evolution of Structures in Dissipative Continuous Systems*, pp. 127. Lecture Notes in Physics m55 (F.H. Busse and S.C. Müller, eds.). Springer-Verlag, Berlin.
- Malomed, B.A., and Nepomnyashchy, A.A. (1990). Kinks and solitons in the generalized Ginzburg-Landau equation. *Phys. Rev. A*, **42**, 6009.
- Moses, E., and Steinberg, V. (1988). Mass Transport in Propagating Patterns of Convection. *Phys. Rev. Lett.*, **60**, 2030.
- Ohlsen, D.R., Yamamoto, S.Y., Surko, C.M., and Kolodner, P. (1990). Transition from Traveling-Wave to Stationary Convection in Fluid Mixtures. *Phys. Rev. Lett.*, **65**, 1431.
- Platten, J.K., and Legros, J.C. (1984). *Convection in Liquids*. Springer-Verlag Berlin.
- Riecke, H. (1992a). Self Trapping of Traveling-Wave Pulses in Binary Mixture Convection. *Phys. Rev. Lett.*, **68**, 301.
- Riecke, H. (1992b). Ginzburg-Landau Equation Coupled to a Concentration Field in Binary Mixture Convection. *Physica*, **D61**, 253.
- Riecke, H. (1996). Solitary Waves under the Influence of a Long-Wave Mode. *Physica*, **D92**, 69.
- Schöpf, W., and Zimmermann, W. (1993). Convection in Binary Fluids: Amplitude Equations, Codimension-2 Bifurcation and Thermal Fluctuations. *Phys. Rev. E*, **47**, 1739.
- Touiri, H., Platten, J.K., and Chavepeyer, G. (1996). Effect of the Separation Ratio on the Transition Between Travelling Waves and Steady Convection in the Two-component Rayleigh-Bénard Problem. *Eur. J. Mech. B/Fluids*, **15**, 241.
- Van Saarloos, W., and Hohenberg, P.C. (1990). Pulses and Fronts in the Complex Ginzburg-Landau Equation near a Subcritical Bifurcation. *Phys. Rev. Lett.*, **64**, 749.
- Veronis, G. (1965). On Finite Amplitude Instability in Thermohaline Convection. *J. Marine Res.*, **23**, 1.
- Walden, R.W., Kolodner, P., Passner, A., and Surko, C.M. (1985). Traveling Waves and Chaos in Binary Fluid Mixtures. *Phys. Rev. Lett.*, **55**, 496.
- Welch, J.E., Harlow, F.H., Shannon, J.P., and Daly, B.J. (1965). The Mac-Method: A Computing Technique for Solving Viscous, Incompressible, Transient Fluid-Flow Problems Involving Free Surfaces. Report LA-3425 Los Alamos Scientific Laboratory of the University of California.
- Winkler, B.L., and Kolodner, P. (1992). Measurements of the Concentration Field in Nonlinear Traveling-Wave Convection. *J. Fluid Mech.*, **240**, 31.
- Zimmermann, G., and Müller, U. (1992). Bénard Convection in a Two-Component System with Soret Effect. *Int. J. Heat Mass Transfer*, **35**, 2245.